

ОБЩАЯ И ФИЗИЧЕСКАЯ ХИМИЯ

UDC 536.46:546.56:546.74

PROCESSING OF COPPER (I) OXIDE WASTE INTO POWDERS OF COPPER AND COPPER-NICKEL ALLOYS BY SCS METHOD

H. A. MAHMOUDI^{1,3}, V. V. VARDAPETYAN¹ and L. S. ABOVYAN²

¹Yerevan State University

A. Manukyan str., 1, Yerevan, AM-0025, Armenia

²A.B. Nalbandyan Institute of Chemical Physics NAS RA,

P. Sevak str., 5/2, Yerevan, 0014, Armenia

³National Iranian Copper Industries Company (NICICO), Kerman, Iran

E-mail: larisa@ichph.sci.am

The possibility of obtaining copper and copper-nickel alloys powders of various compositions by the solution combustion synthesis (SCS) method using copper (I) oxide waste was studied. To achieve complete reduction of metals, combustion laws in the $\text{Cu}(\text{NO}_3)_2\text{-C}_6\text{H}_8\text{O}_7\text{-NH}_4\text{NO}_3$ and $\text{Cu}(\text{NO}_3)_2\text{-Ni}(\text{NO}_3)_2\text{-C}_6\text{H}_8\text{O}_7\text{-NH}_4\text{NO}_3$ systems were investigated at various fuel-to-oxidizer ratio and for different ratios of metal nitrates and ammonium nitrate in the initial mixture. It has been established that powdered copper and copper-nickel alloys of various composition can be obtained by solution combustion synthesis method with using copper (I) oxide waste. Optimum conditions for obtaining powdered copper and copper-nickel alloys with 2/1 and 1/1 ratios have been determined. Under optimal conditions, powders of copper, 2Cu-Ni and Cu-Ni alloys with particle size less than 20 microns were obtained.

Figs. 10, tables 2, references 18.

1. Introduction

In the wiring industry at production of copper wires and cables about 0.6-0.7 wt.% of copper is converted into the waste representing mainly copper (I) oxide [1]. Therewith, on all stages of rolling for decreasing the friction forces of moving details, as well as preventing deep oxidation of the metal, hydrocarbon based mineral oils are used as lubricants. Utilization of such wastes requires reliable methods for their reprocessing back into copper [2,3]. One of the ways for utilization of the oily copper wastes is to remove the oil with a suitable organic solvent and then reduce the oil-free waste to

metallic copper and copper-based alloys. For this purpose, one can use both the traditional furnace methods using carbon or hydrogen as a reducing agent [4-6] and the method of self-propagating high-temperature synthesis (SHS) [7,8] using a combined reducer, e.g. polystyrene [9-11].

In the work [12] copper (I) oxide waste reduction was studied after preliminary removing the oil. It was shown that complete reduction of copper from copper (I) oxide waste in the combustion mode is possible by using the polystyrene (PS)+ammonium nitrate (Nt) mixture as a high caloric additive. Recently complete reduction of copper from the oily copper waste in the combustion mode was performed without preliminary cleaning stage, adding only Nt to the initial mixture [13]. It was supposed that due to its hydrocarbonic nature, the oil can serve as a combined reducer instead of polystyrene for reduction of copper oxide [13].

Another way for utilization of the oil-free copper waste is to convert it to copper nitrate and then reduce the copper nitrate to metallic copper by the solution combustion synthesis (SCS) method [14]. The latter is a specific variety of a more general SHS method [8] and employs exothermic self-propagating reactions in reactive solutions or gels for the preparation of nanoscale oxides, sulfides, nitrides, metals and alloys [14-17].

The reactants in these processes mainly are metal nitrates (oxidizers) and organic compounds (fuels) [14]. The fuel should have a relatively low decomposition temperature ($<600\text{K}$) and high solubility in water. Some fuels can form complexes with metal ions, thus increasing the solubility of the reactants in the solvent. The molecular-level mixing of the multiple metal nitrates ensures the preparation of complex oxides and/or metal alloys with high uniformity for the constituents.

Duration of the SCS process is in the order of minutes, and the maximum temperature could be as high as 2000 K. Solid products of the SCS reactions exhibit porous morphology due to the release of a large volume of gases. The microstructure of the materials depends on the characteristics of the solution before the reaction initiation [14]. In most cases, the products consist of isotropic near-spherical, polyhedral, or irregular-shaped nanoscale crystalline grains of 10-100 nm.

In this work the solution combustion synthesis method was applied for the reduction of: a) copper from copper nitrate and b) joint reduction of copper and nickel from corresponding nitrates to produce fine powders of metallic copper and Cu-Ni alloys in a single step. For increasing the exothermic effect of low caloric oxidizer + fuel reactions and performing joint reduction of both the nitrates to metallic Cu and Ni in combustion mode ammonium nitrate (a strong oxidizer) was applied as well. To achieve this aim, combustion laws in the $\text{Cu}(\text{NO}_3)_2\text{-}\varphi\text{C}_6\text{H}_8\text{O}_7\text{-}x\text{NH}_4\text{NO}_3$ and $\text{Cu}(\text{NO}_3)_2\text{-}k\text{Ni}(\text{NO}_3)_2\text{-}\varphi\text{C}_6\text{H}_8\text{O}_7\text{-}x\text{NH}_4\text{NO}_3$ systems were investigated at various fuel-to-

oxidizer ratio (ϕ) and for different ratios of metal nitrates and ammonium nitrate in the initial mixture.

Adiabatic combustion temperature (T_{ad}) calculations often preceded direct temperature measurements. These calculations were based on a priori assumptions about the compositions of the products. The shortcoming of this approach is that the equilibrium products for a specific system is unknown and largely depend on the reaction temperatures.

Determination of optimal conditions of the process was based on the results of preliminary thermodynamic calculations for the system under study.

2. Materials and methods

Copper waste with 95% particle size less than 1.0 mm, nitric acid with density of 1.35 g/cm³, nickel nitrate hexahydrate, Ni(NO₃)₂·6H₂O (Pure grade, Russia), citric acid, C₆H₈O₇·H₂O (Pure grade, Russia), and granulated porous ammonium nitrate with granule size less than 3 mm (mark B, high grade, GOST 2-85, Russia) were used as the initial reagents.

In this work copper oily waste of wiring industry was used after removing the oil, which according to the XRD analysis represents mainly copper (I) oxide with small amount of metallic copper (Fig. 1). The content of mineral oil (a mixture of various unsaturated and saturated aliphatic and aromatic hydrocarbons, hereinafter C_nH_m) in the copper waste, determined by the mass loss after diethyl ether treatment amounted to 5-10%.

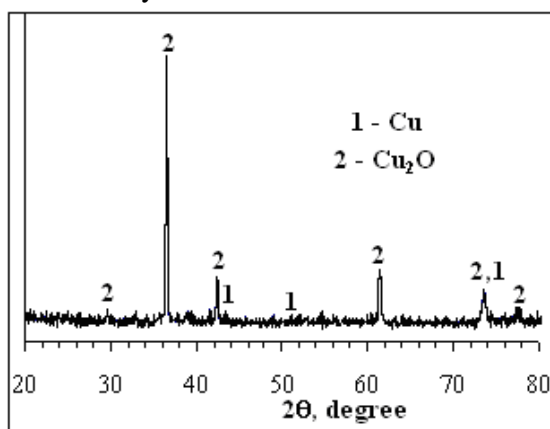


Fig. 1. XRD pattern of the initial copper (I) oxide waste.

In combustion experiments solutions were prepared from the following initial mixtures: $\text{Cu}(\text{NO}_3)_2 + \left(\frac{10}{15}\phi\right)\text{C}_6\text{H}_8\text{O}_7 + x\text{NH}_4\text{NO}_3$, $2\text{Cu}(\text{NO}_3)_2 + \text{Ni}(\text{NO}_3)_2 + \left(\frac{30}{15}\phi\right)\text{C}_6\text{H}_8\text{O}_7 + x\text{NH}_4\text{NO}_3$ and $2\text{Cu}(\text{NO}_3)_2 + 2\text{Ni}(\text{NO}_3)_2 +$

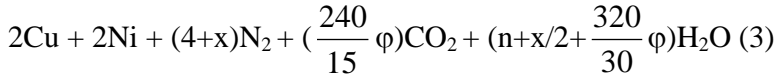
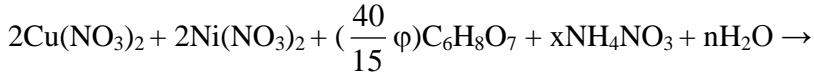
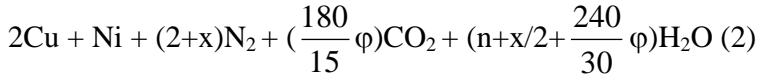
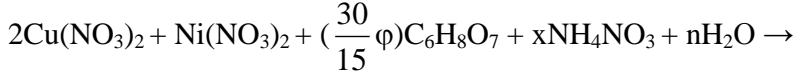
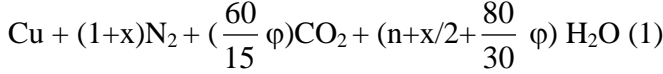
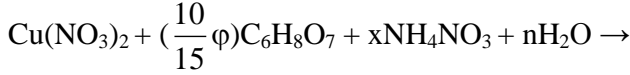
$(\frac{40}{15} \varphi) \text{C}_6\text{H}_8\text{O}_7 + x\text{NH}_4\text{NO}_3$. In the case of $\varphi = 1$ (stoichiometric ratio), the metal nitrate supplies the oxygen required for complete combustion of the fuel, whereas the $\varphi < 1$ or $\varphi > 1$ represent fuel-lean or fuel-rich systems, respectively. Main variables in the combustion experiments were x (moles, ammonium nitrate), and φ (moles, citric acid, $\frac{10}{15}\varphi$, $\frac{30}{15}\varphi$ and $\frac{40}{15}\varphi$, respectively, fuel or reducing agent) values. The saturated solution of copper nitrate necessary for preparation of the general or joint solutions was prepared by dissolving oil-free copper waste in nitric acid. In the first set of experiments, the reactants with different φ ratios were dissolved in deionized water and mixed using a magnetic stirrer. The solutions were then heated on a hot plate to initiate and study the reactions in self-propagating or volume combustion mode. The solutions were preheated to the boiling point of the solvent. The evaporation of water takes a long time and produced a gel-type substance. After evaporation of the solvent, combustion was initiated mainly in the entire volume of the gel.

The maximal combustion temperature, $T_{c(\text{max})}$, and temperature profiles $T(t)$ were measured by two C-type tungsten-rhenium thermocouples with 0.2 mm in diameter, covered with a thin layer of boron nitride. The thermocouples were placed into the sample with depth of 5 mm from the bottom, and 15-20 mm distance from each other. The standard error of measurement for T_c was $\pm 20^\circ\text{C}$. The output signals of thermocouples were transformed by a multichannel acquisition system and recorded by a computer with frequency up to 1 kHz. After cooling the reaction products were extracted from the reactor and crushed into powder. Final products were examined by XRD analysis with monochromatic CuK_α radiation, wavelength 1.54056 Å (diffractometer DRON-3.0, Burevestnik, Russia) operated at 25 kV and 10 mA. To identify the products from the XRD spectra, the data were processed using the JCPDS database. The microstructure of powders was examined and EDS analyses were performed by the scanning electron microscope Prisma E.

2.1. Thermodynamic calculations

Calculations of adiabatic temperatures (T_{ad}) and composition of the equilibrium products for the $\text{Cu}(\text{NO}_3)_2 \cdot y\text{C}_6\text{H}_8\text{O}_7 \cdot x\text{NH}_4\text{NO}_3 \cdot n\text{H}_2\text{O}$, $2\text{Cu}(\text{NO}_3)_2 \cdot \text{Ni}(\text{NO}_3)_2 \cdot y\text{C}_6\text{H}_8\text{O}_7 \cdot x\text{NH}_4\text{NO}_3 \cdot n\text{H}_2\text{O}$ and $2\text{Cu}(\text{NO}_3)_2 \cdot 2\text{Ni}(\text{NO}_3)_2 \cdot y\text{C}_6\text{H}_8\text{O}_7 \cdot x\text{NH}_4\text{NO}_3 \cdot n\text{H}_2\text{O}$ systems, where $y = \frac{10}{15}\varphi$, $\frac{30}{15}\varphi$ and $\frac{40}{15}\varphi$ were performed by “ISMAN-THERMO” software [18]. To determine the equilibrium state, this program searches for the minimum of the Gibbs free energy accounting for the contributions of all initial, possible intermediate

and final reactants. THERMO software contains a database that includes heat capacities (and their temperature dependencies) for possible gaseous and condensed phase products. For revealing the effect of ϕ ratio (changed in the range from 0.25 to 7.5) at different values of the ammonium nitrate (x) and water (n) the following reactions were considered:



The calculations were performed for constant ambient pressure ($P=1$ atm). The calculated T_{ad} and molar quantities of major gases and condensed products (Cu, Ni, Cu_2O , CuO, NiO and C) were plotted as a function of ϕ for different values of parameters n and x ($n=0\div20$ and $x=0\div4$ moles, respectively). The calculations did not exclude the formation of other possible gaseous products, such as CO, NO, H_2 , O_2 , CH_4 and NH_3). The calculation results include the optimal intervals of variation of the studied parameters for the complete reduction of copper and nickel by the amount of a reducing agent (fuel) and a strong oxidizer.

3. Results and discussion

3.1. SCS in the $\text{Cu}(\text{NO}_3)_2 - \left(\frac{10}{15}\phi\right)\text{C}_6\text{H}_8\text{O}_7 - x\text{NH}_4\text{NO}_3 - n\text{H}_2\text{O}$ system

3.1.1. Thermodynamic consideration

The results of thermodynamic calculations for the $\text{Cu}(\text{NO}_3)_2 - \left(\frac{10}{15}\phi\right)\text{C}_6\text{H}_8\text{O}_7 - n\text{H}_2\text{O}$ system demonstrate (Fig. 2) that with increasing the parameter ϕ within the interval of $0.25 \leq \phi \leq 1.0$ the adiabatic combustion temperature increases from 760 up to 1915°C, and then in the range of $1.0 < \phi < 3.15$ decreases to 590°C at $n=0$. For $n=4$ the adiabatic combustion temperature in the same intervals of the parameter ϕ increases from 80 up to 1310°C and then decreases to 510°C. Difference in values (Fig. 2) of T_{ad} is

due to the different phase composition of the both gaseous (CO , CH_4 and NH_3) and condensed (Cu_2O and C) products. In both cases maximum T_{ad} is observed at $\varphi=1$. At that complete reduction of copper for $n = 0$ is observed at the same value of φ ($\varphi=1$) and in the case of $n = 4$ at $\varphi = 1.125$. The growth of T_{ad} is conditioned by increase of the share of the exothermic reaction in the overall process. The amount of reducer (φ) affects also on the phase composition of the products. It is expressed by a change in the amounts and ratios of the formed individual substances in different states of aggregation.

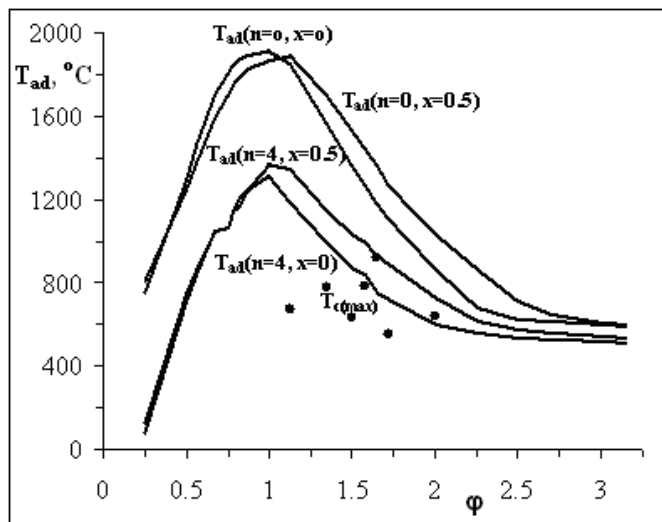


Fig. 2. Calculated combustion temperature (T_{ad}) vs φ ratio for the $\text{Cu}(\text{NO}_3)_2 - \varphi\text{C}_6\text{H}_8\text{O}_7 - n\text{H}_2\text{O} - x\text{NH}_4\text{NO}_3$ system depending on x and n values. The plot includes also experimental data for maximum temperature (data points) for SCS, $x=0$.

The main condensed products are Cu , Cu_2O , CuO and, in some cases, carbon was also formed. Similar thermodynamic calculations were performed for the $\text{Cu}(\text{NO}_3)_2 - (\frac{10}{15}\varphi)\text{C}_6\text{H}_8\text{O}_7 - x\text{NH}_4\text{NO}_3 - n\text{H}_2\text{O}$ system too.

Note that the introduction of a strong oxidizer into the initial mixture affects both the adiabatic temperature and the phase composition of the products. Based on the calculation results optimum areas from thermodynamic point of view for the complete reduction of copper were obtained in the ranges of variation of $\varphi=1\div 2.5$ and $x=0.5\div 1.0$ mole, respectively.

3.1.2. Experimental results

The temperature–time profiles recorded during the experiments at combustion of $\text{Cu}(\text{NO}_3)_2 - (\frac{10}{15}\varphi)\text{C}_6\text{H}_8\text{O}_7 + x\text{NH}_4\text{NO}_3$ mixtures are shown in fig. 3. These curves provide accurate information on both: the ignition and maximum combustion temperature, as well as heating and cooling rates. The

shape of the temperature–time curves is typical for volume combustion processes. After evaporation of the solvent, combustion was initiated in the entire volume of gel, and temperature rapidly rises from the ignition point, T_{ig} , to the maximum value $T_{c(max)}$ followed by the sharp cooling stage.

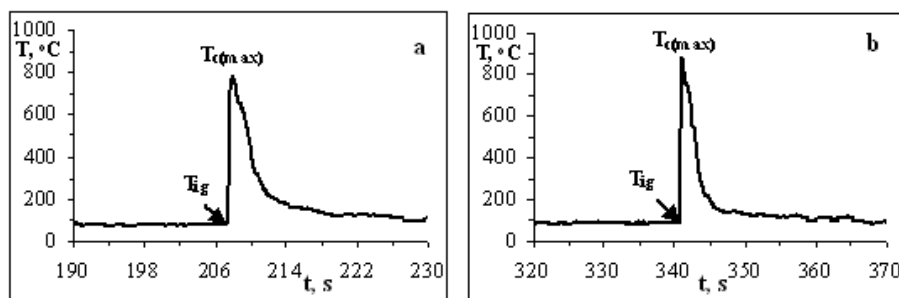


Fig. 3. Typical temperature–time curves at SCS of $\text{Cu}(\text{NO}_3)_2 + \varphi\text{C}_6\text{H}_8\text{O}_7$ (a) and $\text{Cu}(\text{NO}_3)_2 + \varphi\text{C}_6\text{H}_8\text{O}_7 + x\text{NH}_4\text{NO}_3$ (b) mixtures, $\varphi=1.35$, $x=0.5$.

In fig. 4 the results of combustion experiments for the $\text{Cu}(\text{NO}_3)_2 - (\frac{10}{15}\varphi)\text{C}_6\text{H}_8\text{O}_7$ system are demonstrated. As may be seen, for $\varphi > 1$ (fuel-rich mixtures) the maximum combustion temperature increases in the range from $\varphi = 1$ to $\varphi = 1.65$ ($670\text{--}920^\circ\text{C}$) and then for $\varphi > 1.65$ $T_{c(max)}$ decreases (down to 640°C). As a result, for $\varphi > 2.25$, there is no ignition, only isolated point flashes are observed. A similar picture is also observed at $\varphi < 0.75$ (fuel-lean mixtures), which is associated with the partial reduction of copper.

According to XRD analysis results (Fig. 4b) a single-phase product (copper powder) was obtained only in the narrow range of citric acid content ($\varphi = 1.35\text{--}1.43$). For the mixtures in which citric acid is taken in a smaller ($\varphi < 1.35$) or larger ($\varphi > 1.43$) amount, partial reduction is observed: the product contains also copper oxides: Cu_2O and CuO . These results are in disagreement with the results of thermodynamic calculations presented in fig. 2. Such disagreement could be related to the fact that the combustion of solutions containing citric acid proceeds vigorously, accompanied with significant heat loss because of rapid removal of large amount of gaseous products from the reaction zone, as a result of which they do not participate in the establishment of equilibrium.

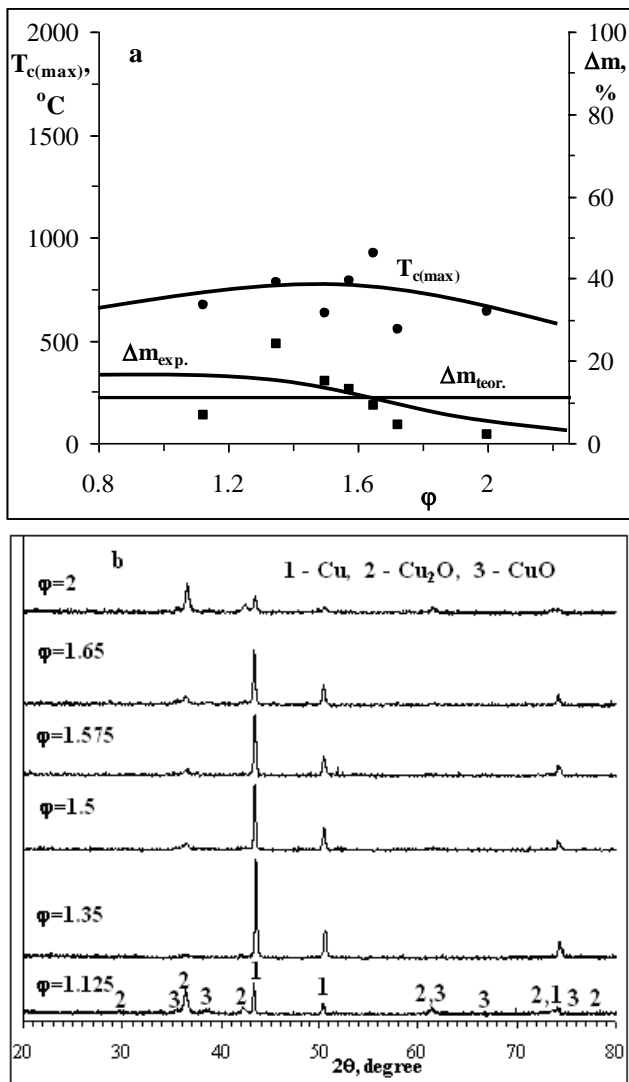


Fig. 4. Maximum combustion temperature ($T_{c(max)}$) and mass loss ($\Delta m_{exp.}$ and $\Delta m_{teor.}$) vs. ϕ for the $Cu(NO_3)_2 + \phi C_6H_8O_7$ mixtures (a) and XRD patterns of combustion products for SCS of the $Cu(NO_3)_2 + \phi C_6H_8O_7$ mixtures at different values of the parameter ϕ (b).

Further studies were carried out in the direction of expanding the range of variation of the parameter ϕ for the complete reduction of copper.

The addition of different amounts of a strong oxidizer (Nt) to the initial mixture influences on the values of $T_{c(max)}$ and Δm , and phase composition of final products. Thus, according to XRD analysis results, complete reduction of copper at addition of $x=0.5$ moles Nt takes place in the range of $1.5 \leq \phi \leq 1.65$. Note that with an increase of the parameter ϕ in the range from 1.125 to 2, the combustion temperature does not change significantly (810–860°C). Introduction of a strong oxidizer for fuel-rich mixtures at $\phi \geq 1.72$ does not ensure complete reduction of copper: the products contain CuO ,

Cu_2O and Cu with varying component ratios. However, with an increase in the amount of a strong oxidizer, an expansion of the ignition region is also observed: e.g. at $x=4$ moles the ignition region for the value of parameter φ ratio expands from 2.25 to 4.5.

Based on the results obtained, it can be concluded that the optimal range by the parameter φ for the complete reduction of copper is $1.5 \leq \varphi \leq 1.65$ at $x=0.5$ mole of Nt. However, the use of citric acid as a fuel does not provide the necessary conditions for obtaining nanoscale copper powder with separated particles. During combustion, an increase in the particle size and the formation of copper agglomerated powder with a particle size less than $20 \mu\text{m}$ is observed.

3.2. SCS in the $2\text{Cu}(\text{NO}_3)_2-k\text{Ni}(\text{NO}_3)_2-\varphi\text{C}_6\text{H}_8\text{O}_7-x\text{NH}_4\text{NO}_3-n\text{H}_2\text{O}$ system. Combustion of this system was studied in a wide range of changing the parameters φ ($0.5 \leq \varphi \leq 7.5$) and x ($0 \leq x \leq 1$) at 2 various ratios of metal nitrates ($k = 1$ & 2). The choice of these compositions is due to the need to obtain Cu-Ni alloys with a ratio of metals: 2:1 and 1:1. For each case the effect of the fuel (citric acid) content and strong oxidizer (Nt) on the combustion laws, phase and chemical composition of the combustion products were studied. Determination of optimal conditions of the process was based on the results of preliminary thermodynamic analysis for the above-mentioned systems.

3.2.1. SCS in the $2\text{Cu}(\text{NO}_3)_2-\text{Ni}(\text{NO}_3)_2-(\frac{30}{15}\varphi)\text{C}_6\text{H}_8\text{O}_7-x\text{NH}_4\text{NO}_3-n\text{H}_2\text{O}$ system. The temperature–time profiles recorded during the experiments at combustion of $2\text{Cu}(\text{NO}_3)_2 + \text{Ni}(\text{NO}_3)_2 + (\frac{10}{15}\varphi)\text{C}_6\text{H}_8\text{O}_7 + x\text{NH}_4\text{NO}_3$ mixtures are shown in fig. 5. As can be seen, the shape of the curves, as in the case of the previous system (Fig. 3), is typical for volume combustion processes.

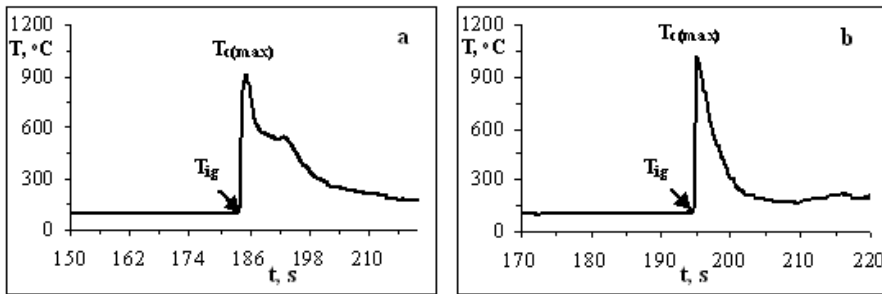


Fig. 5. Typical temperature–time curves at SCS of $2\text{Cu}(\text{NO}_3)_2 + \text{Ni}(\text{NO}_3)_2 + \varphi\text{C}_6\text{H}_8\text{O}_7$ (a) and $2\text{Cu}(\text{NO}_3)_2 + \text{Ni}(\text{NO}_3)_2 + \varphi\text{C}_6\text{H}_8\text{O}_7 + x\text{NH}_4\text{NO}_3$ (b) mixtures, $\varphi=1.95$, $x=1$.

The results of combustion experiments for the $2\text{Cu}(\text{NO}_3)_2-\text{Ni}(\text{NO}_3)_2-\varphi\text{C}_6\text{H}_8\text{O}_7$ and $2\text{Cu}(\text{NO}_3)_2-\text{Ni}(\text{NO}_3)_2-\varphi\text{C}_6\text{H}_8\text{O}_7-x\text{NH}_4\text{NO}_3$ systems are

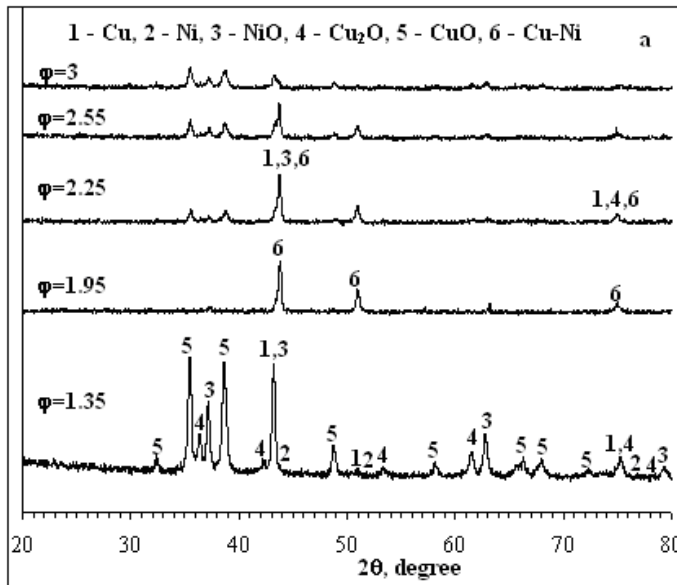
presented in table 1. Note that in the systems under study the lower concentration limit of combustion is observed at $\varphi=0.75$. The results of Table 1 show that with increasing the parameter φ and introduction a strong oxidizer into the initial mixture affects both the maximum combustion temperature and phase composition of the products.

Table 1

Maximum combustion temperature ($T_{c(max)}$) and phase composition of the combustion products for different values of parameters φ and x for the $2Cu(NO_3)_2 + Ni(NO_3)_2 + \varphi C_6H_8O_7 + xNH_4NO_3$ mixtures

φ ($C_6H_8O_7$), mole	x (NH_4NO_3), mole	$T_{c(max)}$, $^{\circ}C$	Phase composition of combustion products
1.35	0	580	CuO, NiO, Cu, Cu_2O
1.95	0	870	Cu-Ni, NiO
1.95	1	860	Cu, NiO, Cu_2O , CuO, Ni
2.55	0	730	Cu-Ni, CuO, NiO
2.55	1	850	Cu-Ni
3	1	750	Cu-Ni, CuO, NiO, Cu_2O , Cu

As can be seen from table 1, according to the XRD analysis results, complete joint reduction of copper and nickel takes place only at $\varphi=1.95$ (stoichiometric ratio, $T_{c(max)}=870^{\circ}C$) for $x=0$ (Fig. 6a) and $\varphi=2.55$ (fuel-rich mixture, $T_{c(max)}=870^{\circ}C$) for $x=1$ (Fig. 6b). In other cases, the product also contains various amounts of metal



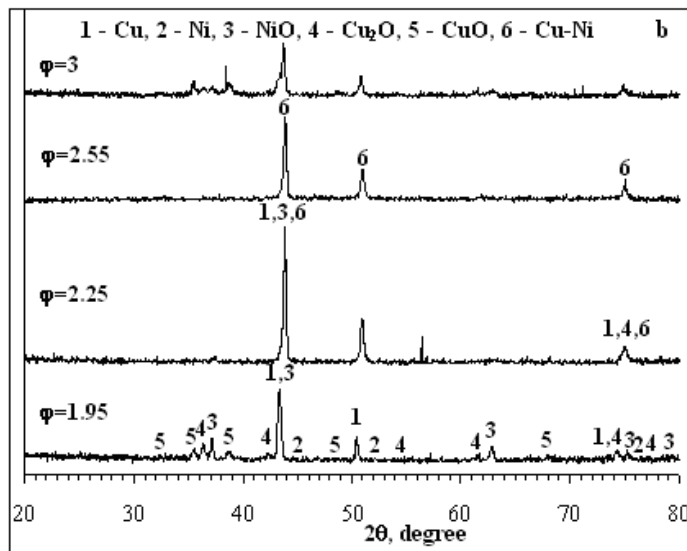


Fig. 6. XRD patterns of the combustion products for SCS of the $2\text{Cu}(\text{NO}_3)_2 + \text{Ni}(\text{NO}_3)_2 + \varphi\text{C}_6\text{H}_8\text{O}_7$ (a) and $2\text{Cu}(\text{NO}_3)_2 + \text{Ni}(\text{NO}_3)_2 + \varphi\text{C}_6\text{H}_8\text{O}_7 + x\text{NH}_4\text{NO}_3$ (b) mixtures for different values of the parameter φ , at $x=1$ oxides: Cu_2O , CuO and NiO . In the case of smaller amounts of citric acid ($\varphi < 1.95$), the oxides are not completely reduced, and in the case of larger amounts ($\varphi > 1.95$), the combustion temperature decreases.

Note that the use of citric acid as a fuel does not provide necessary conditions for obtaining nanoscale copper-nickel alloy powder with molar ratio of 2/1 (32 wt.% of Ni). During the combustion process, an increase in particle size is observed and the formation of Cu-Ni alloy powder with a particle size less than $20\ \mu\text{m}$.

The chemical homogeneity of the 2Cu-Ni alloy was examined by EDS analysis to determine the spatial distribution of metals in the sample. These examinations demonstrate reasonable uniformity of metals along the sample.

3.2.2. SCS in the $2\text{Cu}(\text{NO}_3)_2 - 2\text{Ni}(\text{NO}_3)_2 - (\frac{40}{15}\varphi)\text{C}_6\text{H}_8\text{O}_7 - x\text{NH}_4\text{NO}_3 - n\text{H}_2\text{O}$ system

3.2.2.1. Thermodynamic consideration

The results of thermodynamic calculations for the $2\text{Cu}(\text{NO}_3)_2 - 2\text{Ni}(\text{NO}_3)_2 - (\frac{40}{15}\varphi)\text{C}_6\text{H}_8\text{O}_7$ system demonstrate (Fig. 7) that with increasing the parameter φ within the interval of $0.5 \leq \varphi \leq 3.45$ the adiabatic combustion temperature increases from 30 up to 1895°C and then in the range $3.45 < \varphi < 7.5$ decreases to 885°C at $n=0$. For $n=10$ the adiabatic combustion temperature in the same intervals of the parameter φ increases from 30 up to 1520°C and then decreases to 685°C . Difference in the values (Fig. 7) of T_{ad} is due to the different phase composition of the gaseous (CO , CH_4 and NH_3) and condensed (Cu_2O , CuO and NiO) products. In two cases, for $n = 0$ and $n = 10$ moles, maximum values of T_{ad} and complete joint

reduction of both metals are observed at the value of the parameter φ : $\varphi=3.45$ and $\varphi=4.25$, respectively.

The introduction of a strong oxidizer into the initial mixture affects both the adiabatic temperature and the phase composition of the products. Note that maximum value of T_{ad} and complete co-reduction of metals are observed at different values of the parameter φ , namely at $4.5 \leq \varphi \leq 7.5$ for $x=1$.

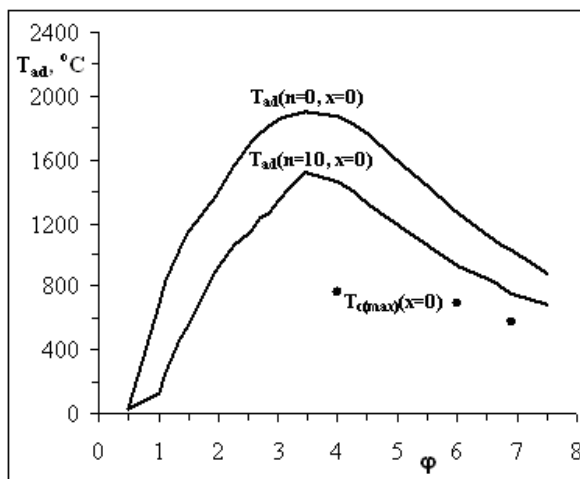


Fig. 7. Calculated combustion temperature (T_{ad}) vs φ ratio for the $2\text{Cu}(\text{NO}_3)_2 - 2\text{Ni}(\text{NO}_3)_2 - \varphi\text{C}_6\text{H}_8\text{O}_7 - n\text{H}_2\text{O}$ system depending on n values. The plot includes also experimental data for maximum temperature (data points) for SCS.

Based on the thermodynamic calculation results, it can be concluded that the optimal ranges of variation by the parameter φ and x for the complete joint reduction of both metals are $\varphi=4.25 \div 7.5$ and $x=0 \div 1.0$ mole, respectively.

3.2.2.2. Experimental results

The results of temperature measurements demonstrate (Fig. 8) that combustion temperature is significantly higher in the presence of ammonium nitrate (Fig. 8b).

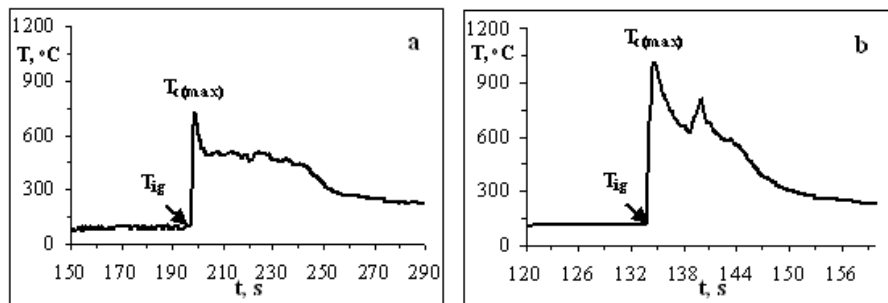


Fig. 8. Typical temperature–time curves at SCS of the $2\text{Cu}(\text{NO}_3)_2 + 2\text{Ni}(\text{NO}_3)_2 + \varphi\text{C}_6\text{H}_8\text{O}_7$ (a) and $2\text{Cu}(\text{NO}_3)_2 + 2\text{Ni}(\text{NO}_3)_2 + \varphi\text{C}_6\text{H}_8\text{O}_7 + x\text{NH}_4\text{NO}_3$ (b) mixtures, $\varphi=3$, $x=1$.

The measured values of the maximum combustion temperature ($T_{c(max)}$) and XRD analysis results of the combustion products are presented in Table 2 and fig. 9.

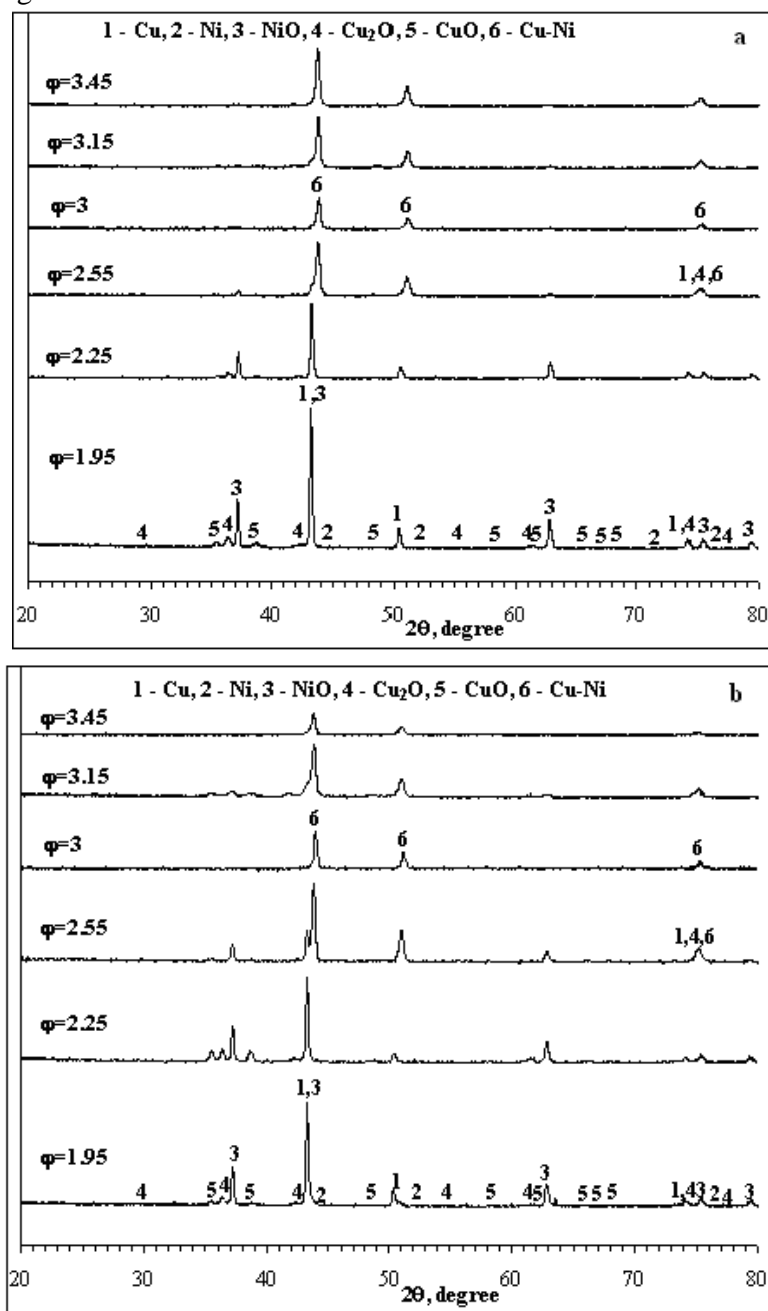


Fig. 9. XRD patterns of the combustion products for SCS of the $2Cu(NO_3)_2 + 2Ni(NO_3)_2 + \varphi C_6H_8O_7$ (a) and $2Cu(NO_3)_2 + 2Ni(NO_3)_2 + \varphi C_6H_8O_7 + xNH_4NO_3$ (b) mixtures for different values of the parameter φ . $x=1$.

Table 2

The maximum combustion temperature ($T_{c(max)}$) and phase composition of the combustion products for different values of the parameters ϕ and x for the $2Cu(NO_3)_2 + 2Ni(NO_3)_2 + \phi C_6H_8O_7 + xNH_4NO_3$ mixtures

ϕ ($C_6H_8O_7$), <i>mole</i>	x (NH_4NO_3), <i>mole</i>	$T_{c(max)}$, °C	Phase composition of combustion products
1.95	0	760	Cu, NiO, Cu_2O , CuO
1.95	1	660	Cu, NiO, Cu_2O , CuO
3	0	700	Cu-Ni
3	1	970	Cu-Ni
3.45	0	580	Cu-Ni, NiO
3.45	1	950	Cu-Ni, Cu, NiO

For the $2Cu(NO_3)_2 - 2Ni(NO_3)_2 - \phi C_6H_8O_7$ and $2Cu(NO_3)_2 - 2Ni(NO_3)_2 - \phi C_6H_8O_7 - xNH_4NO_3$ systems, the lower concentration limit of combustion is observed at a higher value of the parameter ϕ than in the $Cu(NO_3)_2 - \phi C_6H_8O_7 - xNH_4NO_3$ and $2Cu(NO_3)_2 - Ni(NO_3)_2 - \phi C_6H_8O_7 - xNH_4NO_3$ systems, at $\phi = 1.35$.

From the presented diffraction patterns (Fig. 9a, b) for these systems, it can be seen that in both the cases: $x=0$ and $x=1$, a single-phase combustion product is obtained for the same value of the parameter ϕ : $\phi = 3$ (the optimal amount of fuel), representing a monophasic Cu-Ni alloy with 48 wt.% content of Ni.

Based on the results of EDS analyses for the Cu-Ni product (Fig. 10), significantly high chemical homogeneity and uniform distribution of metals in the Cu-Ni alloy powder were observed.

Thus, it has been established that powdered copper and copper-nickel alloys of various compositions can be obtained by the solution combustion synthesis method with using copper (I) oxide waste. It is shown that phase composition of the combustion products can be controlled by changing the amounts of citric acid and ammonium nitrate in the initial mixture. The optimal conditions for obtaining powdered copper and copper-nickel alloys with ratios 2/1 and 1/1 have been determined. Under optimal conditions, powders of copper, 2Cu-Ni and Cu-Ni alloys with particle size less than 20 microns were obtained.

ՊՂՆՁԻ (I) ՕՔՍԻԴԱՅԻՆ ԹԱՓՈՆՆԵՐԻ ՎԵՐԱՄՇԱԿՈՒՄԸ ՊՂՆՁԻ ԵՎ ՊՂԻՆՁ-ՆԻԿԵԼ ՆԱՄԱՉՈՒՎԱԾՔԻ ՓՈՇԻՆԵՐԻ՝ ԼԱՍ ԵՂԱՆԱԿՈՎ

Ն. Ա. ՄԱՏՄՈՒԴԻ, Վ. Վ. ՎԱՐԴԱՊԵՏՅԱՆ և Լ. Ս. ԱԲՈՎՅԱՆ

Ուսումնասիրվել է լուծույթների այրմամբ սինթեզի (ԼԱՍ) եղանակով պղնձի (I) օքսիդային թափոնի վերամշակման և դրանից պղնձի ու պղինձ-նիկել տարբեր բաղադրությամբ համաձուլվածքների փոշիներ ստանալու հնարավորությունը: Մետաղների ամբողջական վերականգնման համար ուսումնասիրվել են այրման օրինաափոխությունները $Cu(NO_3)_2 \cdot C_6H_8O_7 \cdot NH_4NO_3$ և $Cu(NO_3)_2 \cdot Ni(NO_3)_2 \cdot C_6H_8O_7 \cdot NH_4NO_3$ համակարգերում՝ վառելիք-օքսիդիչի (Փ) և մետաղների ու ամոնիումի նիտրատների տարբեր հարաբերակցությամբ ելային խառնուրդներ: Պարզվել է, որ մետաղական պղնձի և տարբեր բաղադրությամբ պղինձ-նիկել համաձուլվածքների փոշիներ կարելի է ստանալ լուծույթների այրմամբ սինթեզի եղանակով՝ օգտագործելով պղնձի (I) օքսիդային թափոնը: Որոշվել են մետաղների նիտրատներից պղնձի և 2/1 ու 1/1 հարաբերակցությամբ պղինձ-նիկել համաձուլվածքների փոշիների ստացման օպտիմալ պայմանները ըստ ելային խառնուրդի բաղադրության: Օպտիմալ պայմաններում ստացվել են 20 միկրոնից փոքր մասնիկների չափսով պղնձի և 2Cu-Ni ու Cu-Ni համաձուլվածքների փոշիներ:

ПЕРЕРАБОТКА ОТХОДОВ ОКСИДА МЕДИ (I) В ПОРОШКИ МЕДИ И МЕДНО-НИКЕЛЕВЫХ СПЛАВОВ МЕТОДОМ СГР

А. А. МАГМУДИ^{1,3}, В. В. ВАРДАПЕТЯН¹ и Л. С. АБОВЯН²

¹ Ереванский государственный университет
Армения, 0025, Ереван, ул. А. Манукяна, 1

² Институт химической физики им. А.Б. Налбандяна НАН РА
Армения, 0014, Ереван, ул. П. Севака, 5/2

³ Национальная иранская медная промышленная компания, Керман, Иран
E-mail: larisa@ichph.sci.am

Исследована возможность получения порошков меди и медно-никелевых сплавов различного состава методом синтеза горением растворов (СГР) с использованием отходов оксида меди (I). Для достижения полного восстановления металлов исследованы закономерности горения в системах $Cu(NO_3)_2 \cdot C_6H_8O_7 \cdot NH_4NO_3$ и $Cu(NO_3)_2 \cdot Ni(NO_3)_2 \cdot C_6H_8O_7 \cdot NH_4NO_3$ при различных соотношениях топливоокислитель, нитратов металлов и аммония в исходной смеси. Установлено, что порошки меди и медно-никелевых сплавов различного состава могут быть получены методом синтеза горения растворов с использованием отходов оксида меди (I). Определены оптимальные условия получения порошков меди и медно-никелевых сплавов с соотношением 2/1 и 1/1 из нитратов металлов. В оптимальных условиях были получены порошки меди, сплавов 2Cu-Ni и Cu-Ni состава с размером частиц менее 20 мкм.

REFERENCES

- [1] Slade M.E. An Econometric Model of the US Copper and Aluminum Industries: How Cost Changes Affect Substitution and Recycling, London: Routledge, 2018, Chapters 3–4.
- [2] Agrawal A., Kumari S., Sahu K.K. // Ind. Eng. Chem. Res., 2009, v. 48, №13, p. 6145.
- [3] Sheih Sh.-W., Tsai M.-Sh. // Waste Manage. Res., 2000, v. 18, №5, p. 478.

- [4] *Handbook of Non-Ferrous Metal Powders. Technologies and Applications*. Oleg D. Neikov, Stanislav S. Naboychenko, Gordon Dowson, Eds., First edition, Amsterdam, Elsevier, 2009, Chapter 16.
- [5] *Lebukhova N.V., Karpovich N.F.* // Inorg. Mater., 2008, v. 44, №8, p. 890.
- [6] *L'vov, B.V.* // Thermochim. Acta, 2000, v. 360, №2, p. 109.
- [7] *Merzhanov A.G.* // Ceramics International, 1995, v. 21, p. 371.
- [8] *Merzhanov A.G.* // J. Mater. Chem., 2004, v. 14, p. 1779.
- [9] *Yamukyan M.H., Manukyan Kh.V., Kharatyan S.L.* // Chem. Eng. J., 2008, v. 137, p. 636.
- [10] *Kharatyan S.L.* / X Intern. Symposium on Self-propagating High-temperature Synthesis, 6-11 July, 2009, Tsakhkadzor, Armenia, Book of Abstracts, p. 62 (2009).
- [11] *Kharatyan S.L.* "Metal powders". In «Concise Encyclopedia of Self-Propagating High-Temperature Synthesis». Ed. by *Inna P. Borovinskaya, Alexander A. Gromov, Evgeny A. Levashov, Yuri M. Maksimov, Alexander S. Mukasyan, Alexander S. Rogachev*, 2017, p. 196.
- [12] *Mahmoudi H.A., Abovyan L.S., Kharatyan S.L.* // Chem. J. of Armenia, 2017, v. 70, №4, p. 477.
- [13] *Mahmoudi H.A., Abovyan L.S., Aydinyan S.V., Kharatyan S.L.* // Int. J. Self-Propag. High-Temp. Synth., 2019, v. 28, №4, p. 233.
- [14] *Varma A., Mukasyan A.S., Rogachev A.S., Manukyan K.V.* // Chem. Rev, 2016, v. 116, p. 14493.
- [15] *Amirkhanyan N., Kharatyan S., Manukyan K., Aprahamian A.* // Combustion and Flame, 2020, v. 221, p. 110.
- [16] *Kumar A., Wolf E.E., Mukasyan A.S.* // AIChE J., 2011, v. 57, p. 2207.
- [17] *Rao G.R., Mishra B.G., Sahu H.R.* // Mater. Lett., 2004, v. 58, p. 3523.
- [18] *Shiryaev A.* // Intern. Journal of SHS, 1995, v.4, №4, p.351.